Resonant inelastic x-ray scattering study of the electronic structure of Cu_2O

Young-June Kim*
Department of Physics, University of Toronto, Toronto, Ontario, Canada M5S 1A7

J. P. Hill
Department of Condensed Matter Physics and Materials Science, Brookhaven National Laboratory, Upton, New York 11973, USA

H. Yamaguchi
Department of Electronics and Information Systems, Akita Prefectural University, 84-4 Ebinokuchi Tsuchiya, Honjo, Akita 015-0055, Japan

T. Gog and D. Casa
XOR, Advanced Photon Source, Argonne National Laboratory, Argonne, Illinois 60439, USA
(Received 24 April 2009; revised manuscript received 23 February 2010; published 4 May 2010)

A resonant inelastic x-ray scattering study of the electronic structure of the semiconductor cuprous oxide, Cu_2O, is reported. When the incident x-ray energy is tuned to the Cu K-absorption edge, large enhancements of the spectral features corresponding to the electronic transitions between the valence band and the conduction band are observed. A feature at 6.5 eV can be well described by an interband transition from occupied states of mostly Cu $3d$ character to unoccupied states with mixed $3d$, $4s$, and O $2p$ character. In addition, an insulating band gap is observed, and the momentum dependence of the lower bound is measured along the Γ-R direction. This is found to be in good agreement with the valence-band dispersion measured with angle-resolved photoemission spectroscopy.

DOI: 10.1103/PhysRevB.81.195202 PACS number(s): 71.20.Nr, 78.70.Ck

I. INTRODUCTION

In recent years, resonant inelastic x-ray scattering (RIXS) has been used as a probe of various types of electronic excitations in many condensed-matter systems.[1] In these studies, when the incident photon energy is tuned to the x-ray absorption edge of interest, the intensity of certain spectral features is greatly enhanced, sometimes by up to a few orders of magnitude. Initially, soft x-ray photons were used to study the electronic structure in semiconductors and insulators.[1] Recently, RIXS at transition metal K edges has also been gaining interest due to the added benefit of the momentum-resolving capability provided by the short wavelength of the hard x-ray photons.[2–5] Such transition metal K-edge RIXS is often called *indirect* RIXS, since the intermediate state does not directly involve $3d$ photoelectrons, unlike RIXS in the soft x-ray regime (transition metal L edges), which is therefore referred to as *direct*.

One of the attractions presented by hard x-ray RIXS is the possibility of its use in studying momentum-resolved electronic structure. In a simple picture of the RIXS cross-section, the momentum-dependent part of the cross-section may be expressed as the joint density of states (JDOS) of the unoccupied and occupied bands for a particular momentum transfer.[1,6,7] In other words, the RIXS spectrum can be regarded as measuring interband transitions at a finite momentum transfer with an appropriate prefactor. Although this viewpoint is probably too simplistic, attempts to develop a linear-response theory for the RIXS cross-section based on this approach have been made.[8–11] For example, in the limit of either very weak or very strong core hole potential, van den Brink and van Veenendaal have shown that the indirect RIXS cross-section is a linear combination of the charge response function and the dynamic longitudinal spin-density correlation function.[9] This line of approach is quite intriguing, since it suggests that one could use RIXS as a tool for reconstructing electronic structure at the finite momentum transfer.[12]

Despite extensive RIXS investigations of strongly correlated cuprate compounds, little work has been done to date to study conventional semiconductors with well-known electronic structure. This is unfortunate, because investigation of well-characterized materials with a known band structure is essential to formulate quantitative understanding of this new experimental technique. In this paper, we present just such an investigation of semiconducting Cu_2O, using Cu K-edge RIXS and show that indirect RIXS can measure the JDOS of this weakly correlated system.

Cuprous oxide, Cu_2O, is a naturally occurring mineral called "cuprite." It is a direct-gap semiconductor with well-characterized exciton lines, which are often considered as textbook examples of Mott-Wannier-type excitons.[13] In particular, Bose-Einstein condensation of the exciton gas has been reported and has drawn much attention over the last two decades.[14,15] In recent years, however, this material has drawn renewed interest due to its potential applications in solar-energy conversion and catalysis.[16] Considerable attention has also been paid to this material due to the unusual O-Cu-O linear bonding.[17]

Cuprous oxide crystallizes in a cubic structure with space group $Pn\bar{3}m$.[18,19] Since Hayashi and Katsuki's measurement of exciton absorption lines,[20] early experimental work on this material focused mostly on optical absorption studies of the different exciton series, and is reviewed in Refs. 21 and 22. Further, the electronic structure of Cu_2O has been studied

using various *ab initio* methods.[23–31] These studies suggest that Cu_2O is a semiconductor with direct band gap, although the calculated gap varies widely among the different approaches and typically disagrees with the experimental value of about 2 eV. (For a comprehensive comparison, see Table I in Ref. 31.)

Advances in core-level spectroscopy techniques developed at synchrotron x-ray sources have made it possible to test some of the earlier predictions concerning the electronic structure of Cu_2O. X-ray absorption studies near copper L edges[32] as well as at the O K edge[33] have been carried out to elucidate the unoccupied bands. Ghijsen *et al.*[34] carried out both x-ray photoemission spectroscopy (XPS) and bremsstrahlung isochromat spectroscopy (BIS) to probe valence-band and conduction-band densities of states, respectively. These experimental results could be largely accounted for with the calculated band structure, confirming that Cu_2O is a conventional band insulator with no, or very weak, electron correlation. The top of the valence band is dominated by Cu d states while the lowest lying conduction band is primarily of d character which hybridizes with Cu $4s$ and $4p$ states and with O $2p$ states.

As a result of the renewed interest in this material, there have been several recent studies of the electronic structure of Cu_2O using state-of-the-art electron spectroscopy techniques. Bruneval *et al.*[30] measured the valence-band dispersion along the Γ-R direction with the angle-resolved photoemission spectroscopy (ARPES) and were able to explain the observed dispersion using a self-consistent GW method, while Önsten *et al.*[35] used high-energy ARPES to measure the valence-band dispersion along the Γ-M direction. Finally, and of particular interest here, Hu *et al.*[31] carried out comprehensive soft x-ray (direct) RIXS studies of Cu_2O and have compared their results with a calculation based on JDOS-like interband transitions.

In this paper, we present a detailed study of Cu_2O using indirect RIXS. In particular, we will focus on the energy region near the band gap and report our measurement of the dispersion relation of the band-gap edge along the Γ-R direction. The observed momentum dependence of the gap edge is consistent with the dispersion of the valence band as observed with ARPES.[30] In addition, we observe another band of excitations at 6.5 eV, which can be explained as interband transitions from the occupied Cu $3d$ state to the unoccupied state, which is a mixture of Cu $3d$, $4s$, and O $2p$. We contrast this with the soft RIXS data of Hu *et al.*[31] Taken together, these results suggest that the indirect (Cu K-edge) RIXS is a good probe of electronic structure, which complements established techniques such as optical spectroscopy and photoemission spectroscopy.

II. EXPERIMENTAL DETAILS

The RIXS experiments were carried out at the Advanced Photon Source on the undulator beamline 9IDB. A double-bounce Si(333) monochromator and a spherical ($R=1$ m), diced Ge(733) analyzer was used to obtain an overall energy resolution of 0.4 eV (full width at half maximum). We also utilized a high-resolution setup with a Si(444) channel-cut secondary monochromator and a diced Ge(733) analyzer with 2 m radius of curvature. This provides an overall energy resolution of 0.13 eV.

A single-crystal sample of Cu_2O was grown using the traveling solvent floating zone method. The details of the crystal growth were reported in Ref. 36. The crystal used in the RIXS measurements came from the same batch as the one used in the optical studies reported in Ref. 37. The as-grown crystal was mechanically polished and etched in order to optimize the surface condition. The crystal was mounted on an aluminum sample holder at room temperature inside an evacuated chamber.

Most of the measurements were carried out near the $\mathbf{Q}=(2,0,1)$ point. The reduced momentum transfer $\mathbf{q}$ is defined as $\mathbf{q}\equiv\mathbf{Q}-\mathbf{G}$, where $\mathbf{G}$ is a reciprocal lattice vector and is measured from the Brillouin zone center. Note that the Cu_2O structure is composed of an interpenetrating fcc lattice of Cu and a bcc lattice of O. Therefore, (h,k,l) reflections with unmixed indices (h,k,l all even or all odd) will have a strong Bragg peak intensity, following the fcc structure factor, while the reflections with mixed indices, but $h+k+l=$even, will have a weak Bragg peak intensity coming from the bcc lattice of oxygen atoms. Reflections with $h+k+l=$odd, such as the (2,0,1) point, are forbidden. However, Eichhorn *et al.*[19] reported intensity at such positions with the incident energy near the Cu K edge, due to the anisotropic Cu environment. As a result, the $\mathbf{q}=0$ point data were, in fact, taken at the (2,0.05,1) position to reduce the background due to the resonant elastic intensity.

III. RESULTS AND DISCUSSION

A. Energy dependence

In Fig. 1, we show representative RIXS scans obtained with different incident photon energies (E_i) as denoted on the left side of the figure. Each scan is taken at the (2,0.05,1) position and plotted as a function of energy loss ($\hbar\omega=E_i-E_f$). In each scan, there is a large zero-energy-loss peak arising from the quasielastic background due to phonons and static disorder. In addition, there is a broad, strong energy-loss feature in the 3–5 eV range. Between these two prominent features, one can observe a sharp edgelike RIXS feature around $\hbar\omega\approx 2$ eV, which exhibits a large resonant enhancement at $E_i=8982.5$ eV.

In general, there are two distinct types of spectral features observed by RIXS. One is a valence-electron excitation that appears at fixed energy loss ($\hbar\omega$) regardless of the incident energy, similar to Raman-scattering peaks. The sharp edgelike feature at 2 eV corresponds to such an excitation. The other type is due to emission lines arising from radiative transitions between atomiclike states, which are observed at fixed final photon energy (E_f). When plotted as a function of energy loss, as shown in Fig. 1, the peak position of the latter features therefore shifts as the incident energy is varied above the edge. The broad feature at higher energy ($\sim$5 eV) in Fig. 1 corresponds to such an emission line.

The sharp edgelike feature shows quite a narrow resonance behavior around the incident energy of $E_i=8982.5$ eV. We note that this energy corresponds to the

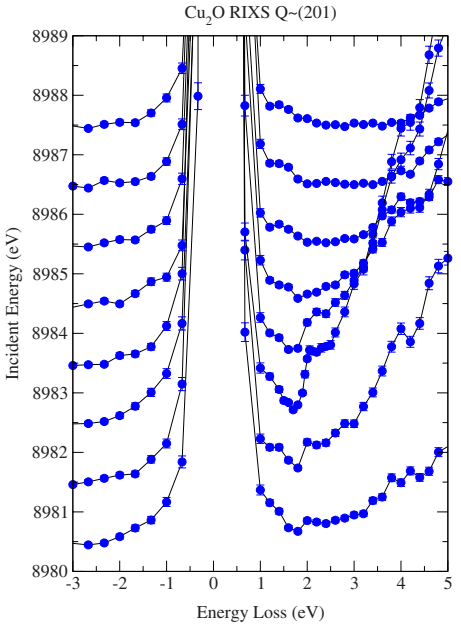

FIG. 1. (Color online) Scattered intensity at $\mathbf{Q} \approx (2\ 0\ 1)$, plotted as a function of energy loss, $\hbar\omega$. The scans are shifted vertically for clarity. The incident energy for each scan can be read off from the vertical axis.

sharp peak in the x-ray absorption spectra shown in Fig. 8 of Ref. 38 and Fig. 8 of Ref. 39. Since this is the strongest absorption feature, we can associate this incident energy, and the corresponding intermediate state of the resonant inelastic process, with the $\underline{1s}4p$ state following a $1s \rightarrow 4p$ dipole transition, where $\underline{1s}$ denotes a $1s$ core hole. Since Cu is found with Cu^{+} valence in Cu_2O, this intermediate state energy is shifted down by about 10 eV compared to the Cu^{2+} state in cuprate materials such as La_2CuO_4.[3] Note that due to the cubic crystal symmetry, no polarization dependence of this excitation is expected for the crystal as a whole. We identify this sharp edgelike feature as the $\mathbf{q}=0$ band gap, since its energy loss of $\hbar\omega \approx 2$ eV coincides with the optical gap energy. As we will see in the next section, this identification is corroborated by the momentum dependence of this feature.

In addition to this low-energy feature at the band gap, there are higher energy features, which are observed for wide range of incident energies. In Fig. 2, we show an intensity map as a function of both incident energy and energy loss again taken at (2,0.05,1). Note that the incident energies used in Fig. 2 are higher than those for the data shown in Fig. 1. One can clearly identify a very broad and strong spectral feature located at around $\hbar\omega \approx 6.5$ eV, which is resonantly enhanced over a wide range of incident energies; most notably around $E_i = 8995$ and 9000 eV. In addition, there is a weak low-energy feature located around $\hbar\omega \approx 4$ eV that resonates around $E_i = 8999$ eV. In Fig. 3, scans obtained with $E_i = 8995.5$ and 9000.5 eV are plotted, which illustrate that the peak position of the loss features does not vary much with the incident energy. The high intensity above the main peak at 6.5 eV is due to an emission line discussed above.

To understand the origin of these excitations, it is useful to consider the electronic density of states. Using both XPS

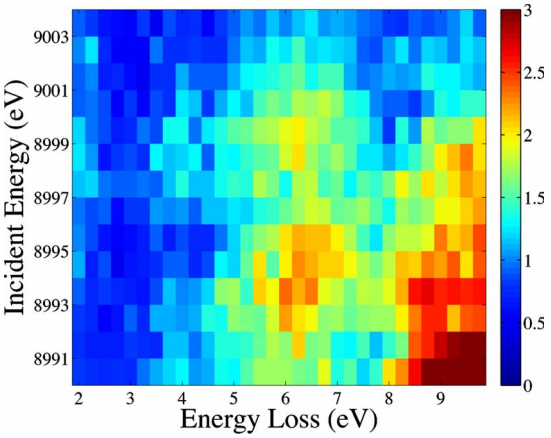

FIG. 2. (Color online) Scattered intensity at $\mathbf{Q} \approx (2\ 0\ 1)$, plotted in pseudocolor intensity map. The horizontal axis is energy loss and the vertical axis the incident photon energy. The intensity scale bar is shown on the right. Note that the incident energies are higher than those in Fig. 1.

and BIS techniques, Ghijsen *et al.*[34] reported valence-band and conduction-band densities of states for Cu_2O. The most prominent peak in BIS occurs around 3 eV above the Fermi level, while XPS shows a large peak centered around 3 eV below the Fermi level with shoulders on both sides. The densities of states based on these XPS and BIS results are shown schematically in Fig. 4(a). The main peak in the XPS spectra is mainly of Cu d character, while the larger binding-energy shoulder, at about 7 eV below the Fermi level, has mainly O $2p$ character (based on the various calculations).[25,26,34] The nature of the low-lying unoccupied states has been attributed to mixed Cu $3d$-O $2p$ states[34] or to Cu $4s$ states.[26] Given this picture, it is natural to associate the $\hbar\omega = 6.5$ eV RIXS feature with the transition from the $3d$ to either Cu $3d$-O $2p$ mixture or $4s$. Note that this RIXS peak around 6.5 eV is more or less independent of the incident energy over a very wide range. Then the higher energy RIXS feature at 9–10 eV presumably is due to the transition from the occupied O $2p$ to empty $3d$ or $4s$ states.

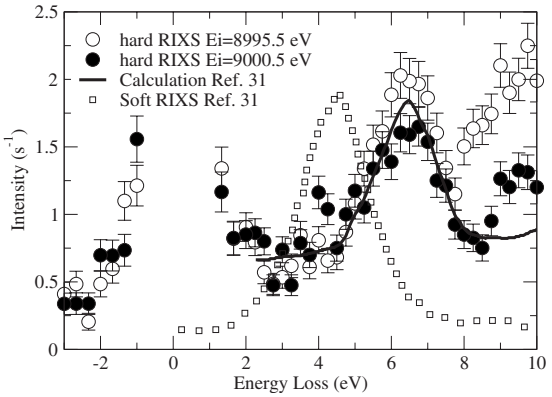

FIG. 3. Energy-loss scan obtained with $E_i = 8995.5$ and 9000.5 eV. The momentum is $\mathbf{Q} \sim (2\ 0\ 1)$. The open circles are experimental soft x-ray RIXS spectrum from Ref. 31. The solid line is a calculated RIXS spectrum from Ref. 31 scaled to match the current data.

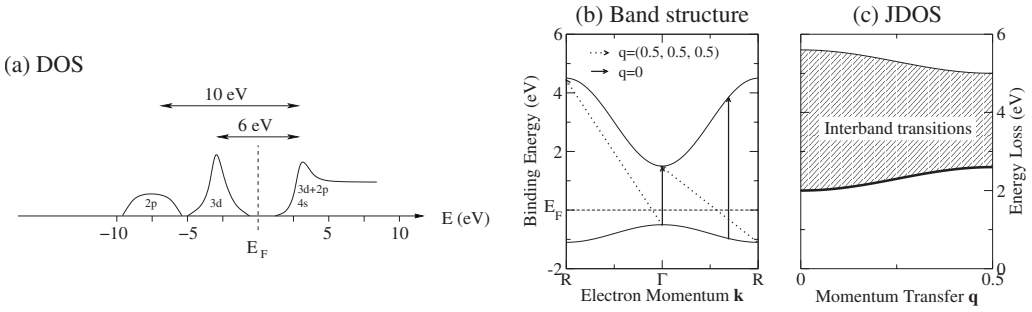

FIG. 4. (a) Schematic representation of experimental DOS from Ref. 34. The states shown here are mostly Cu states, except for the O $2p$ states. (b) Simplified band structure shown for illustrative purposes as described in the text. The arrows denote possible interband transitions with different momentum transfers. Vertical solid lines are $\mathbf{q}=0$ transitions; dashed lines correspond to $\mathbf{q}=(1/2,1/2,1/2)$ transitions. (c) Momentum dependence of the JDOS arising from the band structure shown in (b). Note that the magnitude of the momentum dependence of the lower bound of the interband transition continuum (thick solid line) mimics that of the valence band.

To make a more quantitative comparison, the hard RIXS scans are compared with the calculated spectrum, taken from Ref. 31, in Fig. 3. Hu *et al.*[31] computed the inelastic x-ray scattering intensity due to dipole-allowed interband transitions between filled and empty partial densities of states. The most dominant loss structure is found around 6.5 eV through the $3d \rightarrow 4s/3d$ channels, while there exist weaker features at 4 and 10 eV in the other channels ($4s \rightarrow 4s/3d$). Since the matrix elements for the K-edge experiments are unknown, we plot simply the dominant $3d \rightarrow 4s$ transition (solid line) without any matrix element weighting in Fig. 3. Note that using $3d \rightarrow 3d$ channel also gives the same result. We find it describes the main peak at 6.5 eV remarkably well. Note that neither the peak position nor the core-hole broadening (1.35 eV) has been altered from the calculation in Ref. 31, and only the intensity scale has been changed. On the other hand, the Cu L_3 RIXS spectrum obtained with E_i=933.75 eV in Ref. 31 exhibits a very different shape with an energy-loss feature centered around 4.5 eV, as shown in Fig. 3 (open circles). Hu and co-workers used a phenomenological excitonic density of states in order to account for this discrepancy. This was an *ad hoc* approach that used the experimental L-edge absorption spectrum (for which there is a $2p$ core hole in the final state) in place of the calculated occupied DOS. This was labeled the "excitonic DOS." Although there is no $2p$ core hole in the L-edge RIXS final state, such "excitonic DOS" was required to explain the experimental observations. Figure 3 shows that no such *ad hoc* corrections are required to explain the K-edge RIXS data, which are well reproduced by the theoretical JDOS. Thus, the present comparison suggests that Cu K-edge RIXS (often called indirect RIXS) can measure band structure directly, unlike Cu L_3-edge RIXS. Note that the additional features observed at 4 and 10 eV in the K-edge RIXS could also be explained by the $4s \rightarrow 3d$ transition according to the calculation.[31]

B. Momentum dependence

We now turn to the 2 eV feature. With the incident energy fixed at E_i=8982.5 eV, we studied the momentum dependence of the sharp edge feature observed at 2 eV (Fig. 1). In Fig. 5, we plot the RIXS spectra obtained at **Q** positions along the Γ-R line, that is, with **q** along the $(1,\bar{1},1)$ direction. We plot only a narrow frequency range, in order to emphasize the evolution of the lowest energy excitation as a function of momentum transfer. (Note that there appears to be a small peak at $\hbar\omega \sim 1-1.5$ eV. However, this feature is present in all scans and has no E_i dependence, nor is it observed in the high-resolution data, as shown in the inset of Fig. 5. Thus, it is most likely due to an experimental artifact, presumably due to imperfect fabrication of the spherical analyzers or the background arising from the kapton window of the sample cell, and we do not discuss it further.)

The lowest energy excitation across the band gap shows quite a dramatic momentum dependence. In order to show the dispersion of this excitation graphically, we plot the intensity as a function of $\hbar\omega$ and q in Fig. 6. The intensity

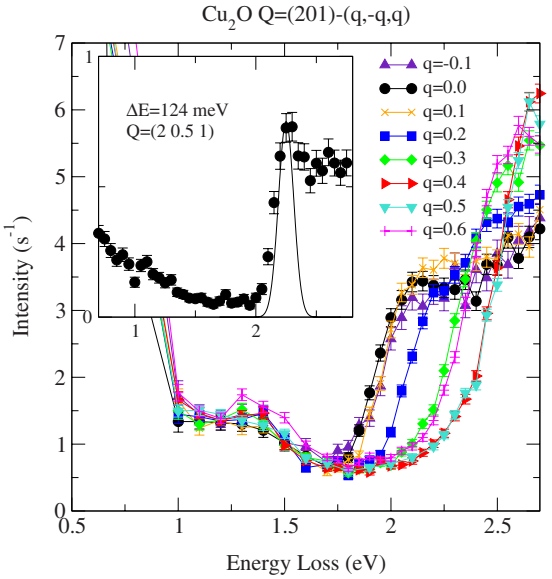

FIG. 5. (Color online) RIXS intensity at different Q positions obtained with fixed incident energy at E_i=8982.5 eV. The Q positions are along the Γ-R line in reciprocal space, that is, along the $(1,\bar{1},1)$ direction. The inset shows the high-resolution data. The resolution function of 124 meV full width is shown as a solid line. Note that the weak feature at 1.3 eV observed in the main figure is an experimental artifact and is not observed in the high-resolution data.

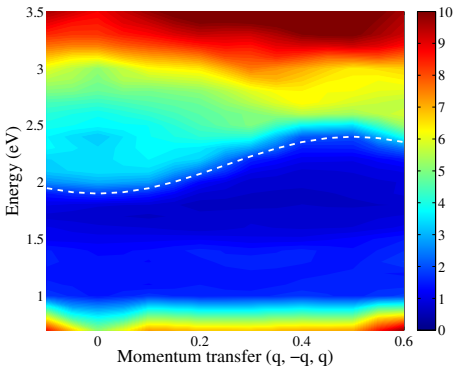

FIG. 6. (Color online) Intensity color map as a function of energy and momentum transfer. The intensity scale in counts per second is shown on the right-hand side of the main figure. Intensity of ten counts per second or higher is shown in brown. The dashed line is an empirical dispersion relation $2.15-0.25\cos(2\pi q)$.

scale is shown on the right-hand side and is described in the figure caption. The boundary between the high-intensity region and the background forms a sinusoidal dispersion relation of the form $\hbar\omega \approx 2.15-0.25\cos(2\pi q)$, as shown as the white dashed line in Fig. 6.

If one adopts the simple view that the RIXS spectrum in a weakly correlated system is proportional to the JDOS at a given momentum transfer, then the observed dispersion in Fig. 6 should reflect the momentum dependence of the lower bound for interband transitions. In order to understand this, let us consider a simple sinusoidal conduction and valence band with a direct gap located at the Γ position. An idealized representation of such a band structure is shown in Fig. 4(b) as a function of electron momentum **k** along the Γ-*R* direction. Here the valence-band dispersion $E_v(k)$ is taken from the recent ARPES data[30] while the conduction-band dispersion $E_c(k)$ is taken from the calculation in Ref. 26.

Finite **q** interband transitions can be represented as vectors connecting two points on the E_v and E_c curves as shown in Fig. 4(b). The frequency and momentum of a particular transition satisfies $\hbar\omega(\mathbf{q})=E_c(\mathbf{k}_p)-E_v(\mathbf{k}_h)$ and $\mathbf{q}=\mathbf{k}_p-\mathbf{k}_h$, where $\mathbf{k}_p$ and $\mathbf{k}_h$ are particle and hole momenta, respectively. Examples of the $\mathbf{q}=0$ transition are shown in solid lines, while the dotted line represents examples of the $\mathbf{q}=(\frac{1}{2},\frac{1}{2},\frac{1}{2})$ transition. Integrating over all possible $\mathbf{k}_p$ and $\mathbf{k}_h$ combinations, one can obtain the **q** dependence of interband transitions along the $(1,\bar{1},1)$ direction. This is shown for this simplified one-dimensional band structure in Fig. 4(c). Since the conduction bandwidth is much larger than the valence bandwidth in this case, the *lower bound* of interband transitions is dominated by the valence band. In other words, the lower bound transitions involve exciting electrons from all $\mathbf{k}_h$ positions of the valence band to the bottom of the conduction band ($\mathbf{k}_p=0$), since it takes more energy to excite electrons into finite $\mathbf{k}_p$ states in conduction band. Therefore, we expect the dispersion of the valence band to be similar to the dispersion of the gap observed in our RIXS measurements. This expectation is borne out by the recent ARPES studies by Bruneval *et al.*[30] and Önsten *et al.*[35] In particular, the valence-band dispersion along the Γ-*R* direction was reported in Ref. 30, which has the valence-band maximum at the Γ position and bandwidth of about 0.6 eV as shown in Fig. 4(b). This is very similar to the bandwidth 0.5 eV observed in Fig. 6. Though, we should note that the picture considered in Fig. 4(b) is an oversimplification in one dimension, and in order to make a quantitative comparison, one would have to take into account the full three-dimensional band structure.

IV. CONCLUSIONS

A RIXS study of the electronic structure of cuprous oxide, Cu_2O, is reported. By tuning the incident x-ray photon energy to the Cu *K*-absorption edge, resonantly enhanced electronic transitions are observed. Comparison with Cu L_3-edge RIXS spectrum and a calculation based on band-structure density of states clearly illustrates that the indirect RIXS spectrum of Cu_2O obtained at the Cu *K* edge can be explained simply by interband transitions. We also observe that the momentum dependence of the lowest energy interband transitions along the Γ-*R* direction and show that it can be well described by the dispersion of the valence band of Cu 3*d* character. Since our measurements were all carried out at room temperature, we could not study exciton physics in this compound, which is an interesting future research topic.

Our main result is that the indirect RIXS cross-section seems to be described by interband transitions from the occupied valence band to the unoccupied conduction band. This gives credence to theoretical efforts to connect the RIXS cross-section with the charge correlation function[9] and also allows one to use indirect RIXS to investigate the electronic structure of materials. This last point is an important one, since RIXS has many advantages over other electron spectroscopy techniques, such as bulk-sensitivity, element-sensitivity, and momentum-resolving capability.

ACKNOWLEDGMENTS

We would like to thank J. van den Brink, W. Ku, and M. van Veenendaal for invaluable discussions. We also thank H. Gretarsson for the help with Fig. 2. The work at University of Toronto was supported by Natural Sciences and Engineering Research Council of Canada. The work at Brookhaven was supported by the U.S. DOE, Office of Science Contract No. DE-AC02-98CH10886. Use of the Advanced Photon Source was supported by the U.S. DOE, Office of Science, Office of Basic Energy Sciences, under Contract No. W-31-109-ENG-38.

*yjkim@physics.utoronto.ca

[1] A. Kotani and S. Shin, Rev. Mod. Phys. **73**, 203 (2001).
[2] M. Z. Hasan, E. D. Isaacs, Z. X. Shen, L. L. Miller, K. Tsutsui, T. Tohyama, and S. Maekawa, Science **288**, 1811 (2000).
[3] Y. J. Kim, J. P. Hill, C. A. Burns, S. Wakimoto, R. J. Birgeneau, D. Casa, T. Gog, and C. T. Venkataraman, Phys. Rev. Lett. **89**, 177003 (2002).
[4] Y. J. Kim *et al.*, Phys. Rev. Lett. **92**, 137402 (2004).
[5] K. Ishii *et al.*, Phys. Rev. Lett. **94**, 207003 (2005).
[6] W. Schulke, *Electron Dynamics by Inelastic X-Ray Scattering* (Oxford University Press, New York, 2007).
[7] Y.-J. Kim, J. P. Hill, S. Wakimoto, R. J. Birgeneau, F. C. Chou, N. Motoyama, K. M. Kojima, S. Uchida, D. Casa, and T. Gog, Phys. Rev. B **76**, 155116 (2007).
[8] T. Nomura and J.-i. Igarashi, Phys. Rev. B **71**, 035110 (2005).
[9] J. van den Brink and M. van Veenendaal, Europhys. Lett. **73**, 121 (2006).
[10] L. J. P. Ament, F. Forte, and J. van den Brink, Phys. Rev. B **75**, 115118 (2007).
[11] M. Takahashi, J. Igarashi, and T. Nomura, J. Phys. Soc. Jpn. **77**, 034711 (2008).
[12] In the case of a system with broad bands, dynamic structure factor $S(\mathbf{q},\omega)$ can be obtained from JDOS. See H. Ehrenreich and M. H. Cohen, Phys. Rev. **115**, 786 (1959), and also Ref. 6.
[13] C. Kittel, *Introduction to Solid State Physics*, 7th ed. (Wiley, New York, 1995).
[14] D. W. Snoke, J. P. Wolfe, and A. Mysyrowicz, Phys. Rev. Lett. **59**, 827 (1987).
[15] J. P. Wolfe, J. L. Lin, and D. W. Snoke, *Bose-Einstein Condensation* (Cambridge University Press, Cambridge, 1995), pp. 281–329.
[16] L. Gou and C. Murphy, Nano Lett. **3**, 231 (2003).
[17] J. M. Zuo, M. Kim, M. O'Keeffe, and J. C. H. Spence, Nature (London) **401**, 49 (1999).
[18] R. Restori and D. Schwarzenbach, Acta Crystallogr., Sect. B: Struct. Sci. **42**, 201 (1986).
[19] K. Eichhorn, A. H. Kirfel, and K. F. Fischer, Z. Naturforsch., A: Phys. Sci. **43**, 391 (1988).
[20] M. Hayashi and K. Katsuki, J. Phys. Soc. Jpn. **5**, 380B (1950).
[21] S. Nikitine, *Optical Properties of Solids* (Plenum, New York, 1969), p. 197.
[22] E. F. Gross, Nuovo Cimento **3**, 672 (1956).
[23] J. P. Dahl and A. C. Switendick, J. Phys. Chem. Solids **27**, 931 (1966).
[24] L. Kleinman and K. Mednick, Phys. Rev. B **21**, 1549 (1980).
[25] W. Y. Ching, Y. N. Xu, and K. W. Wong, Phys. Rev. B **40**, 7684 (1989).
[26] E. Ruiz, S. Alvarez, P. Alemany, and R. A. Evarestov, Phys. Rev. B **56**, 7189 (1997).
[27] X. Nie, S. H. Wei, and S. B. Zhang, Phys. Rev. B **65**, 075111 (2002).
[28] R. Laskowski, P. Blaha, and K. Schwarz, Phys. Rev. B **67**, 075102 (2003).
[29] A. Filippetti and V. Fiorentini, Phys. Rev. B **72**, 035128 (2005).
[30] F. Bruneval, N. Vast, L. Reining, M. Izquierdo, F. Sirotti, and N. Barrett, Phys. Rev. Lett. **97**, 267601 (2006).
[31] J. P. Hu, D. J. Payne, R. G. Egdell, P.-A. Glans, T. Learmonth, K. E. Smith, J. Guo, and N. M. Harrison, Phys. Rev. B **77**, 155115 (2008).
[32] S. L. Hulbert, B. A. Bunker, F. C. Brown, and P. Pianetta, Phys. Rev. B **30**, 2120 (1984).
[33] M. Grioni, J. F. van Acker, M. T. Czyžyk, and J. C. Fuggle, Phys. Rev. B **45**, 3309 (1992).
[34] J. Ghijsen, L. H. Tjeng, J. van Elp, H. Eskes, J. Westerink, G. A. Sawatzky, and M. T. Czyzyk, Phys. Rev. B **38**, 11322 (1988).
[35] A. Önsten, M. Månsson, T. Claesson, T. Muro, T. Matsushita, T. Nakamura, T. Kinoshita, U. O. Karlsson, and O. Tjernberg, Phys. Rev. B **76**, 115127 (2007).
[36] T. Ito, H. Yamaguchi, K. Okabe, and T. Masumi, J. Mater. Sci. **33**, 3555 (1998).
[37] T. Ito, T. Kawashima, H. Yamaguchi, T. Masumi, and S. Adachi, J. Phys. Soc. Jpn. **67**, 2125 (1998).
[38] F. W. Lytle, R. B. Greegor, and A. J. Panson, Phys. Rev. B **37**, 1550 (1988).
[39] J. Guo, D. E. Ellis, G. L. Goodman, E. E. Alp, L. Soderholm, and G. K. Shenoy, Phys. Rev. B **41**, 82 (1990).